Noncontact deep level photo-thermal spectroscopy: Technique and application to semi-insulating GaAs Wafers

Jun Xia and Andreas Mandelis[a)]
Center for Advanced Diffusion-Wave Technologies (CADIFT), Department of Mechanical and Industrial Engineering, University of Toronto, Toronto, Ontario, M5S 3G8, Canada

(Received 18 October 2006; accepted 3 January 2007; published online 9 February 2007)

A purely optical deep level photothermal spectroscopy has been developed for the defect-state characterization of semi-insulating (SI) GaAs wafers. The methodology utilizes near infrared sub-band-gap absorption to monitor the thermal emission of traps after an optical filling pulse, and the data are analyzed in a rate-window manner by a lock-in amplifier. The technique has been applied to a vertical-gradient-freeze grown SI-GaAs wafer, and the very first results are presented. © *2007 American Institute of Physics*. [DOI: 10.1063/1.2437686]

Deep level transient spectroscopy (DLTS), first introduced by Lang,[1] is a powerful tool for detection and characterization of deep defects in semiconductors. Conventional DLTS requires a depleted region and measures the capacitance change after an electrical or optical pulse. This method, however, cannot be applied to high resistivity materials, since the Debye-Huckel length is too large (several millimeters for semi-insulating GaAs at 300 K) and typically exceeds sample dimensions. An alternative technique, known as photoinduced transient spectroscopy (PITS),[2] has been developed by measuring the photocurrent transient in the sample. PITS does not require the preparation of *p-n* junctions, but an electrical contact is still needed. In addition to the intrinsic errors that may be induced by this contact, it makes the technique to be intrusive and hence not practicable for the direct probing of materials for integrated circuit processes.

During the past few years, several noncontact techniques have been developed,[3,4] however, these techniques tend to be quite restrictive in their application scope. For instance, laser-microwave deep level transient spectroscopy (LM-DLTS) requires, for detection, the presence of free carrier concentrations within limits determined to be[3] $8.3\times10^{10}\leqslant n\leqslant 2.6\times10^{13}$ cm^{-3}. Furthermore, the spatial resolution of LM-DLTS is limited by the microwave probe-beam spot size (on the order of 10–20 mm).

In this letter an all optical deep level photo-thermal spectroscopy (DLPTS) is introduced. In DLPTS the free carrier concentration and occupancy of deep levels are monitored by means of optical absorption of a sub-band-gap laser beam. Taking advantage of the purely optical operation and the high spatial resolution of the focused laser spot size (~0.1 mm), DLPTS provides flexible noncontact characterization of deep levels in high resistivity materials.

In DLPTS, the thermal recovery of carriers after excitation is monitored by a sub-band-gap laser. When the laser impinges on the sample, two kinds of absorption occur: one is the free carrier absorption (fca) and the other is the deep level (defect) absorption (dla).

For GaAs, in the near infrared region, the fca is mainly associated with interband absorption, which is caused by the excitation of electrons to a higher conduction band minimum. In the midinfrared region, the fca is mainly caused by interaction with phonons in a semiconductor.[5] Usually, the absorption coefficient α_{fca} is larger at longer wavelengths.[5] In a given wavelength, α_{fca} is proportional to the free carrier density, which can be expressed by $\alpha_{\mathrm{fca}}=\sigma_{\mathrm{fca}}n(t)$ cm^{-1}, where σ_{fca} is the absorption cross section, which could be considered constant in a small temperature range $\Delta T(\sim 150$ K).

dla absorption is caused by injection of carriers from a deep level to the conduction band. This absorption has been commonly applied in the mapping of deep levels in semiconductors, for instance, the EL2 level in semi-insulating GaAs.[6,7] The dla absorption coefficient can be written as $\alpha_{\mathrm{dla}}=\sigma_{\mathrm{dla}}n_T$ cm^{-1}, where σ_{dla} could also be considered a constant.

The absorption can be measured in both transmission and backscattered reflections. In the backscattered reflection case, the raw DLPTS signal is proportional to[6]

$$I(t)=\frac{(1-R)^2S\exp(-2\alpha d)}{1-RS\exp(-2\alpha d)}, \tag{1}$$

where R is the reflection coefficient, S is the scattered reflection coefficient, and d is the sample thickness. Since the absorption coefficient for sub-band-gap laser radiation is very small in SI GaAs, Eq. (1) can be simplified to

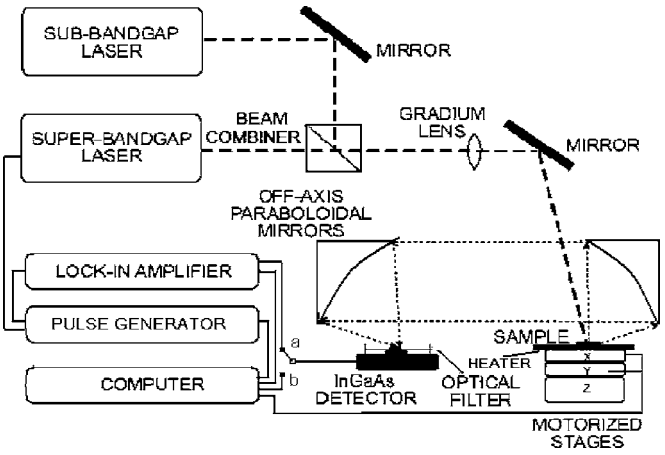

FIG. 1. Schematic diagram for deep level photothermal spectroscopy (DLPTS).

[a)]Electronic mail: mandelis@mie.utoronto.ca

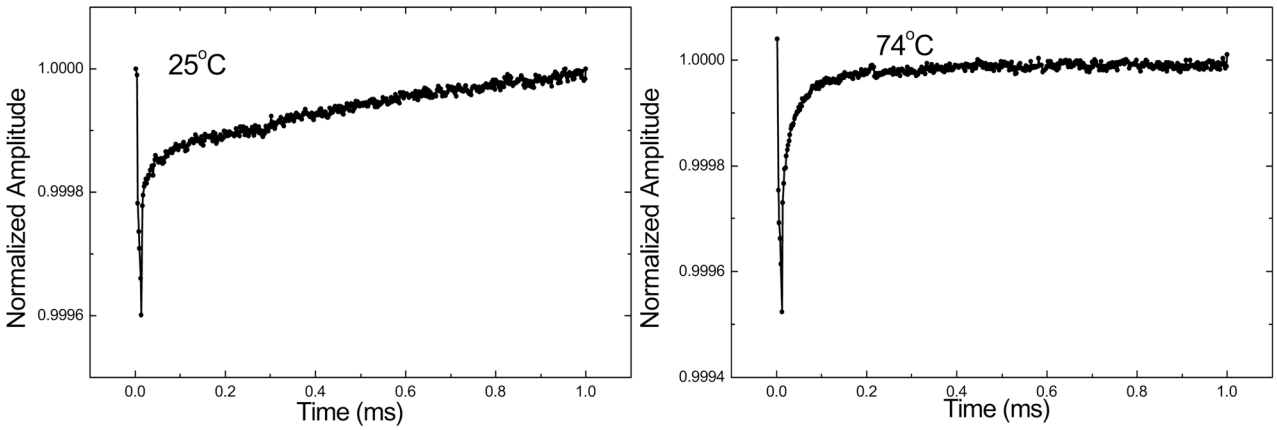

FIG. 2. DLPTS time transients at various temperatures.

$$I(t) \approx \frac{(1-R)^2 S(1-2\alpha d)}{1-RS} \equiv K(1-2\alpha d),$$

$$K \equiv \frac{(1-R)^2 S}{1-RS}. \tag{2}$$

Based on the foregoing absorption mechanisms, the final DLPTS signal can be expressed as

$$I(t) = K[1 - 2\sigma_{\mathrm{fca}} n(t) d - 2\sigma_{\mathrm{dla}} n_T(t) d], \tag{3}$$

where $n(t)$ and $n_T(t)$ have been calculated in PITS measurements based on rate equations assuming a single deep level, and neglecting the retrapping of carriers, as well as the hole capture and emission.[8] The simplified solutions are

$$n(t) = g_{\mathrm{op}} \tau (1 - e^{-t/\tau}), \quad t \leqslant t_p, \tag{4}$$

$$n_T(t) = \frac{N_T}{1 + e_n/(g_{\mathrm{op}} \tau C_n)} (1 - e^{-(nC_n + e_n)t}), \quad t \leqslant t_p, \tag{5}$$

$$n(t) = M[e^{-(t-t_p)e_n} - e^{-(t-t_p)/\tau}] + n(t_p) e^{-(t-t_p)/\tau}, \quad t \geqslant t_p, \tag{6}$$

$$n_T(t) = n_T(t_p) e^{-e_n (t-t_p)}, \quad t \geqslant t_p, \tag{7}$$

where g_{op} is the optical generation rate of free carriers, τ is the lifetime of free carriers, N_T is the density of the deep level, C_n is the capture coefficient of the deep level, $n_T(t_p)$ is the density of occupied states at the end of the filling pulse given in Eq. (5), and $M \equiv n_T(t_p) e_n / (\tau^{-1} - e_n)$. $e_n(T)$ is the thermal emission rate given by $e_n = \gamma_n \sigma T^2 \exp(-E_n/kT)$, where γ_n is a material constant and σ is the electronic capture cross section by the deep level. Substituting in Eq. (3) yields

$$I(t) = K\left[1 - 2\sigma_{\mathrm{fca}} g_{\mathrm{op}} \tau (1 - e^{-t/\tau}) d - 2\sigma_{\mathrm{dla}} \frac{N_T}{1 + e_n/(nC_n)} (1 - e^{-(nC_n + e_n)t}) d\right], \quad t \leqslant t_p, \tag{8}$$

$$I(t) = K\{1 - 2\sigma_{\mathrm{fca}}[M(e^{-(t-t_p)e_n} - e^{-(t-t_p)/\tau}) + n(t_p) e^{-(t-t_p)/\tau}] d - 2\sigma_{\mathrm{dla}} n_T(t_p) e^{-e_n (t-t_p)} d\}, \quad t \geqslant t_p, \tag{9}$$

The schematic diagram of the DLPTS system is shown in Fig. 1. The sample is placed on a temperature controlled heating plate, which allows maintaining constant temperature in the 25–250 °C range or can provide temperature ramping. The excitation source is a periodic super-band-gap laser pulse ($\lambda = 830$ nm) emitting 20 mW (peak power) with a beam diameter in about 0.1 mm. The pulse parameters are controlled by a pulse generator, with the pulse width fixed at 1% of the repetition period. Due to the high absorption coefficient of the super-band-gap beam ($\alpha \sim 10^4$ cm^{-1}), the pump laser penetrates only a few micrometers in the wafer. The probe beam is from a coincident sub-band-gap dc laser ($\lambda = 1550$ nm) emitting 3 mW in about 0.15 mm diameter spot size. The probe laser penetrates the whole wafer and is partly scattered by the rough back surface of the sample. The scattered light is collected by two collimating off-axis paraboloidal mirrors and focused on an InGaAs photodetector with a 1550 nm bandpass filter. For temperature-scanned DLPTS (switch a), the signal is fed into an AMETEK 5210 lock-in amplifier, which functions as a rate window. For time-scanned DLPTS (switch b), the raw signal is collected through a National Instruments PCI-6281 data acquisition (DAQ) card, which has been installed in the computer. Samples used in this work are one-side-polished vertical-gradient-freeze (VGF)-grown SI-GaAs wafers supplied by AXT Inc. The wafers have a resistivity of $(7.2–7.7) \times 10^7\ \Omega$ cm and an EL2 concentration around 10^{16} cm^{-3}.

Figure 2 shows the raw DLPTS transient at several temperatures. After each pulse, there is a rapid increase in the signal accompanied by a slow one. Based on Eq. (9) the fast portion is caused by the $e^{-(t-t_p)/\tau}$ term, while the slow one is caused by $e^{-e_n(t-t_p)}$. As the temperature increases, the slow transient becomes faster, which is consistent with Eq. (9). Based on the proportion between the amplitudes of the fast and slow transients, we can assume $\sigma_{\mathrm{dla}} = \sigma_{\mathrm{fca}}$.

Figure 3 shows the rate-window DLPTS spectrum at various pulse repetition frequencies. At each frequency, there is a single peak in the amplitude channel of the thermal spectrum. The peak height decreases as the frequency increases. This is caused by the decrease in pulse width, which reduces the number of injected carriers. The phase in the spectrum has a negative peak at each frequency, and the peak moves to higher temperatures as frequency increases. Unlike the DLPTS amplitude, the peak-to-trough phase shift does not change much as the frequency increases. This behavior is consistent with the carrier density-wave phase independence from the carrier flux (proportional to the laser intensity).

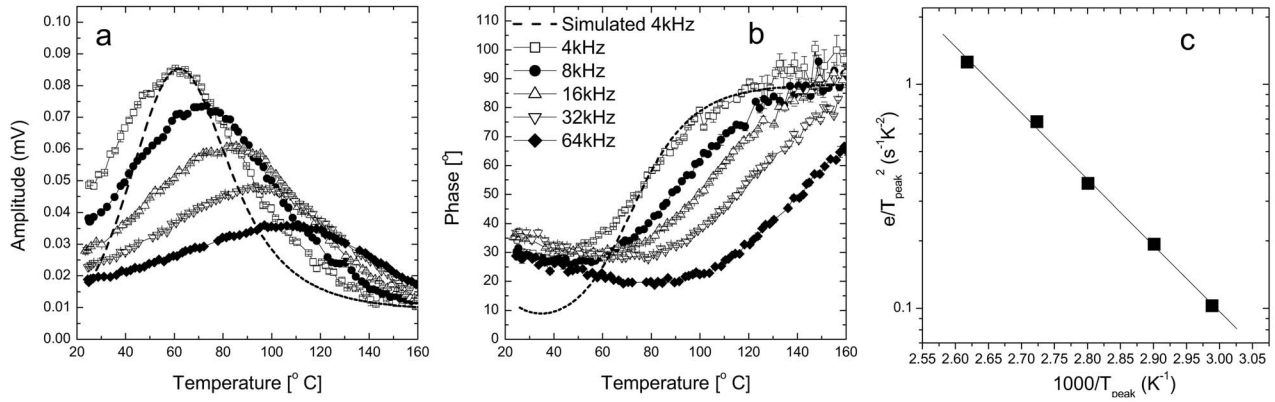

FIG. 3. DLPTS thermal spectrum at various pulse repetition frequencies; (a) amplitude and (b) phase, and (c) Arrhenius plot of the peaks shown in a.

The peak position of the amplitude R can be calculated by the following equation:

$$\frac{dR}{dT} = \frac{dR}{de_n}\frac{de_n}{dT} = 0 \Rightarrow \frac{dR}{de_n} = 0. \tag{10}$$

Based on the assumption that $\sigma_{\mathrm{dla}} = \sigma_{\mathrm{fca}}$, a numerical solution of Eq. (10) gives

$$e_n = 2.869\omega, \tag{11}$$

where ω is the pulse repetition angular frequency.

From this equation, the thermal emission rate at each peak temperature $T_{\mathrm{peak}}(\omega)$ can be calculated. Since $e_n(T) = \gamma_n \sigma T^2 \exp(-E_n/kT)$ and T_{peak} is a function of the pulse repetition frequency, plotting $\log_{10}(e_n/T_{\mathrm{peak}}^2)$ vs $1000/T_{\mathrm{peak}}$ yields a straight line, as shown in Fig. 3. The slope of the line gives the trap activation energy $E_n = 0.59 \pm 0.015$ eV and the intercept at $T = \infty$ gives the capture cross section $\sigma = 2.7 \times 10^{-13}$ cm^2. Based on the energy levels characterized in PITS measurements,[8] $E_{\mathrm{EL3}} = 0.59$ eV and $\sigma_{\mathrm{EL3}} = 1 \times 10^{-13}$ cm^2 identify this peak as corresponding to the EL3 level. This level has been found in many undoped SI-GaAs wafers, and is usually assumed to be an oxygen related defect.[9]

To further examine the validity of the approximate theory, we simulated a temperature scan DLPTS based on the above parameters, and the result is shown in Fig. 3. The simulated curves have the same profile as the experimental curves as well as the same peak position. However, the amplitude is narrower than the experimental one and the phase curve also shows discrepancies in its details. Similar phenomena have already been observed in PITS measurements,[10] which use the same one-level solution. The reason for this is the oversimplifications used in solving the rate equations, such as neglecting the hole emission and capture processes, and the temperature dependent background free carrier concentration, as well as overlapping defect levels.[9] Several improvements of the theory have been introduced during the past few years,[11] but the theoretical transient still results in a simple exponential form unlike the experimental observations. We are currently working on a more comprehensive theory by solving the optical and thermal rate equations adiabatically in different time domains, which allows a solution without neglecting any terms.

The DLPTS technique has been applied to other VGF wafers from ATX, and all of them exhibited the same thermal spectra in both amplitude and phase. However, when applied to n-type GaAs wafers, DLPTS exhibited no peaks in the same above room-temperature range. This is likely due to the domination of absorption by free carriers which masks the kinetic effects of thermal ejection from occupied deep levels. Further low-temperature experiments are under way to investigate shallower levels in SI GaAs and n-GaAs. In conclusion, a purely optical DLPTS methodology has been developed and proved to be a powerful technique for defect-state characterization of SI GaAs. Since both excitation and detection are achieved optically, there is good prospect for DLPTS to be developed to a remote, fully noncontact, process quality control diagnostic for real-time *in situ* characterization of SI-GaAs wafer native and process-induced deep-level defects.

The support of the Natural Sciences and Engineering Research Council of Canada (NSERC) through a Discovery Grant to one of the authors (A.M.) is gratefully acknowledged.

[1] D. V. Lang, J. Appl. Phys. **45**, 3023 (1974).
[2] Ch. Hurtes, M. Boulou, A. Mitonneau, and D. Bois, Appl. Phys. Lett. **32**, 821 (1978).
[3] Y. Fujisaki, Y. Takano, and T. Ishiba, Jpn. J. Appl. Phys., Part 2 **25**, L874 (1986).
[4] J. Lagowski, P. Edelman, and A. Orawski, Semicond. Sci. Technol. **7**, A211 (1992).
[5] A. S. Jordan, J. Appl. Phys. **51**, 2218 (1980).
[6] P. Dobrilla and J. S. Blakemore, J. Appl. Phys. **58**, 208 (1985).
[7] G. M. Martin, Appl. Phys. Lett. **39**, 747 (1981).
[8] D. C. Look, in *Semiconductors and Semimetals*, edited by R. K. Willardson and A. C. Beer (Academic, New York, 1983), Vol. 19, P. 75.
[9] P. Kaminski and R. Kozlowski, Mater. Sci. Eng., B **91–92**, 298 (2002).
[10] J. C. Abele, R. E. Kremer, and J. S. Blakemore, J. Appl. Phys. **62**, 24322 (1987).
[11] M. J. S. P. Brasil and P. Motisuke, J. Appl. Phys. **68**, 3370 (1990).